



Natural Resources
Canada

Ressources naturelles
Canada

**GEOLOGICAL SURVEY OF CANADA
OPEN FILE 8279**

**Epidote associated with the porphyry Cu-Mo
mineralization at the Gibraltar deposit, south-central
British Columbia**

C.H. Kobylinski, K. Hattori, A. Plouffe, and S.W. Smith

2017



Canada 



GEOLOGICAL SURVEY OF CANADA OPEN FILE 8279

Epidote associated with the porphyry Cu-Mo mineralization at the Gibraltar deposit, south-central British Columbia

C.H. Kobylinski¹, K. Hattori¹, A. Plouffe², and S.W. Smith³

¹ Department of Earth and Environmental Sciences, University of Ottawa, 25 Templeton Street, Ottawa, Ontario

² Geological Survey of Canada, 601 Booth Street, Ottawa, Ontario

³ Taseko Gibraltar, 10251 Gibraltar Mine Road, McLeese Lake, British Columbia

2017

© Her Majesty the Queen in Right of Canada, as represented by the Minister of Natural Resources, 2017

Information contained in this publication or product may be reproduced, in part or in whole, and by any means, for personal or public non-commercial purposes, without charge or further permission, unless otherwise specified.

You are asked to:

- exercise due diligence in ensuring the accuracy of the materials reproduced;
- indicate the complete title of the materials reproduced, and the name of the author organization; and
- indicate that the reproduction is a copy of an official work that is published by Natural Resources Canada (NRCan) and that the reproduction has not been produced in affiliation with, or with the endorsement of, NRCan.

Commercial reproduction and distribution is prohibited except with written permission from NRCan. For more information, contact NRCan at nrcan.copyrightdroitdauteur.nrcan@canada.ca.

Permanent link: <https://doi.org/10.4095/305912>

This publication is available for free download through GEOSCAN (<http://geoscan.nrcan.gc.ca/>).

Recommended citation

Kobylinski, C.H., Hattori, K., Plouffe, A., and Smith, S.W., 2017. Epidote associated with the porphyry Cu-Mo mineralization at the Gibraltar deposit, south-central British Columbia; Geological Survey of Canada, Open File 8279, 1 .zip file. <https://doi.org/10.4095/305912>

Epidote associated with the porphyry Cu-Mo mineralization at the Gibraltar deposit, south-central British Columbia

Christopher Kobylinski¹, Keiko Hattori¹, Alain Plouffe², Scott Smith³

¹ *Department of Earth and Environmental Sciences, University of Ottawa, 25 Templeton St., Ottawa, ON K1N 6N5*

² *Geological Survey of Canada, 601 Booth Street, Ottawa, ON K1A 0E8*

³ *Taseko Gibraltar, 10251 Gibraltar Mine Rd., McLeese Lake, British Columbia, V0L 1P0*

Abstract: The Gibraltar porphyry-copper molybdenum deposit in the Canadian Cordillera is hosted by the late Triassic, Granite Mountain Batholith (GMB). The batholith is tonalitic and composed of quartz, plagioclase and minor hornblende and biotite in various modality. The rocks in the batholith show phyllic and propylitic alteration. Propylitic alteration (green rock alteration) is characterised by epidote, chlorite, albite, and is extensive throughout the batholith. The name epidote is used in this paper for epidote group minerals which include clinozoisite, epidote (*sensu stricto*), allanite, ferriepidote and ferriallanite. Epidote occurs as dissemination, isolated grains, and aggregates, and forms mono-mineralic veins and epidote-bearing veins in the batholith. These veins (>2 cm in width) in the batholith generally strike towards the mineralized centre. Epidote enclosed by chalcopyrite or pyrite is compositionally homogeneous and Fe-poor, suggesting that Fe is preferentially incorporated into sulphides and that epidote crystallized together with sulphide minerals. Individual grains of epidote in epidote-bearing veins show compositional zoning with Fe-poor cores and Fe-rich rims. Epidote grains disseminated in the batholith show similar compositional zoning with Fe-poor cores and Fe-rich rims. Allanite and REE-rich epidote are identified in the GMB less than 2 km from mineralization and within the Burgess Creek Stock (10 km from mineralization). Epidote containing 0.01 -1 wt.% REEs is common in grains forming aggregates throughout GMB. Epidote with high REEs (> 1 wt.% REEs) occurs only in rocks with a bulk composition >70 ppm REEs. Compositional zoning of epidote suggests that the hydrothermal history of the GMB comprised of early S-rich hydrothermal activity, followed by S-poor barren hydrothermal activity. Epidote in the Nicola volcanics and Cuisson Lake Unit near the GMB is homogeneous and Fe-rich and commonly contains inclusions of apatite and titanite. The contents of REEs in epidote in the Nicola volcanics are all below the detection limits of SEM (1000 – 5000 ppm) and EPMA (La, 470 ppm; Ce, 380 ppm; Pr, 640 ppm; Nd, 330 ppm).

Introduction

Porphyry Cu mineralization is accompanied by extensive alteration within the host rocks and surrounding country rocks (e.g. Sillitoe, 2010). Propylitic alteration associated with Cu-mineralization produces chlorite, albite and epidote and is called green rock alteration. It can extend a few kilometers from mineralization centres. These alteration minerals can be disseminated in the host and country rocks. Epidote can also form veins and veinlets far from the deposits. Furthermore, epidote is also a common alteration mineral in a variety of rocks

that are not related to porphyry Cu-Mo mineralization. Our objective is to identify the textural and chemical characteristics of epidote associated with porphyry Cu mineralization so that it can be used as an indicator mineral in detrital sediments (e.g. till) to detect propylitic alteration associated with Cu porphyry mineralization. This study on epidote is centred on the Gibraltar porphyry Cu-Mo deposit, the second largest open pit Cu mine in Canada. The deposit is hosted in the late Triassic Granite Mountain Batholith (GMB), which intruded the Nicola Group mafic volcanic rocks of the Quesnel

terrane. Epidote is common within the batholith and abundant in the Nicola volcanic rocks. Furthermore, the Cretaceous Sheridan Creek Stock, which is barren and in contact with the GMB, contains abundant epidote. This paper presents the occurrence and composition of epidote group minerals in the ore zone of the Gibraltar deposit, the GMB, the Nicola volcanic rocks, the Cuisson Lake Unit, and the Sheridan Creek Stock.

Regional geology

Cache Creek terrane

The GMB was recently interpreted as intrusions in the Quesnel terrane close to the border with the Cache Creek terrane to the west (Schiarizza, 2014). Rocks of the Cache Creek terrane underlie the eastern and southern part of the study area (Fig. 1). At a regional scale, it comprises chert, limestone and basalt. Only limestone and chert are present within the study area and these rocks do not contain epidote.

Quesnel terrane

The Quesnel terrane, a volcanic arc terrane, extends along the length of the Canadian Cordillera from central Yukon to the southern limit of British Columbia (Colpron and Nelson, 2011). The Quesnel Terrane is in large part represented by Middle and Upper Triassic submarine volcanic and volcanoclastic rocks, which are assigned to the Takla Group in northern and central British Columbia and to the Nicola Group in the south. The terrane is characterized by pyroxene-phyric basalt, and alkaline to calc-alkaline intrusions (Schiarizza, 2015). The Quesnel terrane is bounded by the oceanic Slide Mountain terrane to the east and the oceanic Cache Creek terrane to the west (Schiarizza, 2015). In the southern Quesnel terrane, intrusive rocks form four linear belts of alternating calc-alkaline and alkaline plutons, younging to the east, and many are accompanied by base metal mineralization (Schiarizza, 2015).

Nicola Group

The volcanic rocks of the Nicola Group are mostly pale green, fine to medium grained tuffs and matrix-supported lapilli tuff breccias of basaltic to andesitic

compositions (Schiarizza, 2015). The Nicola Group also contains intercalated siliclastic sedimentary rocks that are dominated by laminated mudstone-siltstone and lesser medium-grained volcanic sandstone (Schiarizza, 2015).

Geology of the study area

The bedrock geology in the region of the Gibraltar deposit was mapped by Ash et al. (1999b) and more recently by Schiarizza (2014; 2015). The classification of the bedrock units presented below is based on his mapping.

Cuisson Lake Unit (formerly Ash Metamorphic Unit)

The Cuisson Lake Unit, consisting mainly of chlorite schist, limestone and skarn, forms a narrow belt in the southwestern part of the study area, between the GMB and the Sheridan Creek Stock (Figs. 1 and 2). Most rocks in the unit are well foliated and recrystallized, such that primary mineralogy and texture are not preserved (Schiarizza, 2015). Ash et al., (1999a) interpreted the unit as an intensely deformed and recrystallized mafic phase of the GMB. This interpretation led to the old name Ash Metamorphic Unit. Schiarizza (2015) describes the Cuisson Lake Unit as feldspathic volcanoclastic rocks intercalated with limestone which he correlates to the Nicola Group. Volcanic rocks of the Cuisson Lake Unit exposed along the east side of Gibraltar Mine Road, 4 km south of the mine are dark green, fine grained, chloritized and contain abundant epidote (> 40 vol.%). They are similar in appearance to the Nicola volcanic rocks in the northern part of the study area but their bulk composition is slightly different. Mafic rocks of the Cuisson Lake Unit contain less SiO₂ (40.19 wt.% compared to 50.37-51.81 wt%), similar Fe₂O₃(t) (11.35 wt.% compared to 9.18-13.32 wt.%), and higher CaO (27.01 wt.% compared to 8.2-8.6 wt.%) than the Nicola volcanic rocks. High CaO is explained by abundant calcite veinlets (Fig. 2). In the northern part of the study area (Figs. 1 and 2), Nicola volcanics are mingled with limestone. It is possible that the limestone belong to the adjacent Cache Creek Group and that the Cuisson Lake Unit in the southern section of the study area is a metamorphic product of these mingled rocks.

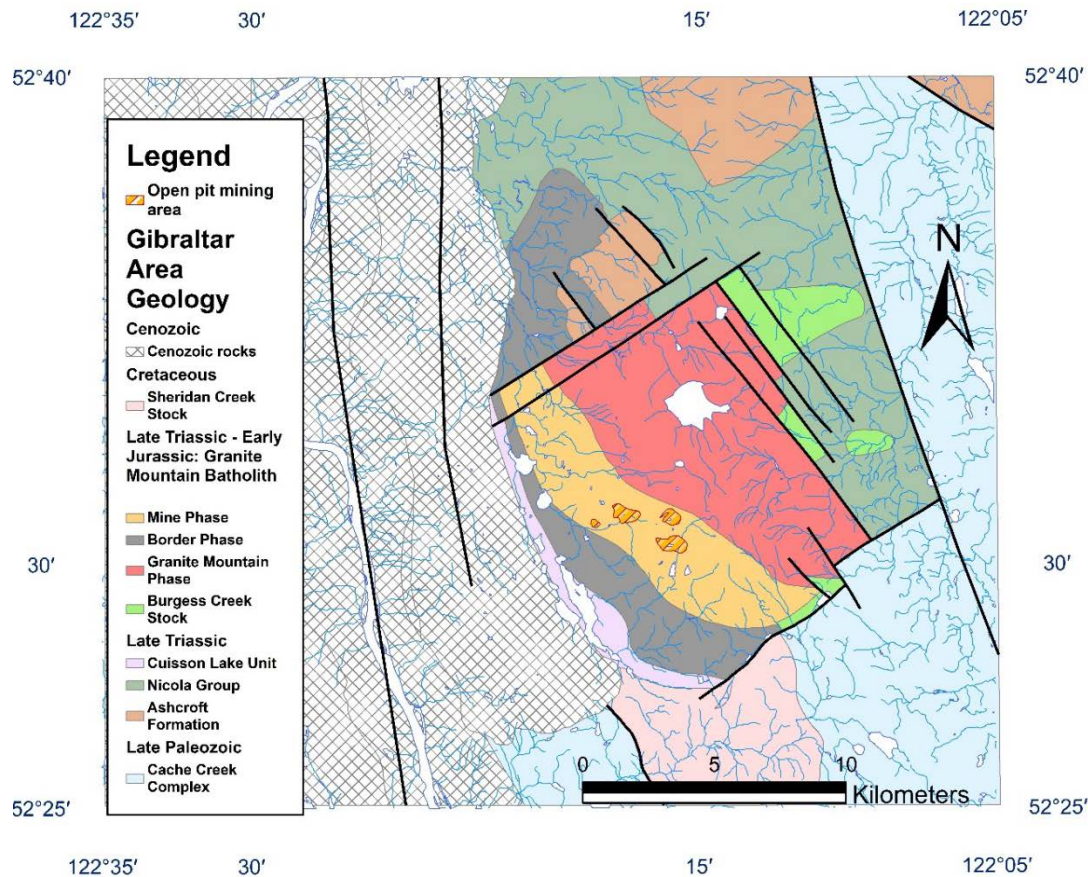


Figure 1. Geological map of the study area, modified from Plouffe and Ferbey (2015). Names of the phases and units within the study area taken from Schiarizza (2015).

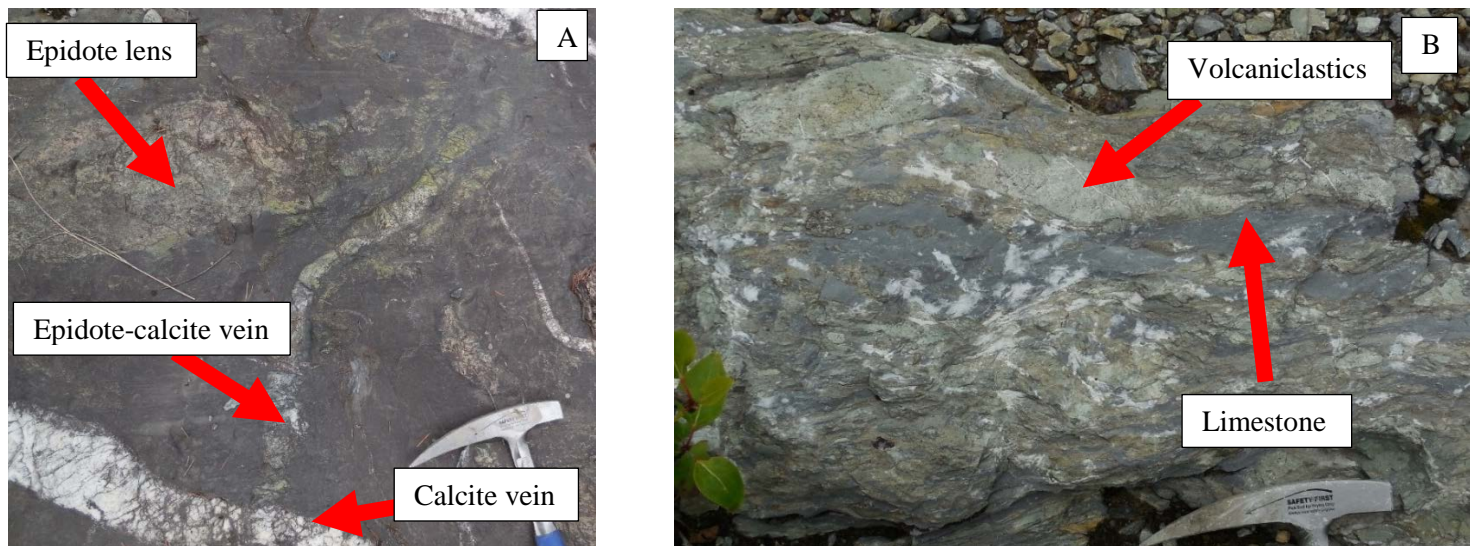


Figure 2. Outcrop photographs with rock hammer for scale. (A) The Cuison Lake Unit along Gibraltar Mine road (Easting 0547384 Northing 5814942 (NAD 83, Zone 10 N)) with deformed veins of epidote, epidote-calcite and calcite and a dark green fine-grained matrix. (B) Outcrop of Nicola volcanic rocks (Easting 0549808 Northing 5829201 (NAD 83, Zone 10 N)) north of the GMB, showing green volcaniclastic rock and blue-grey limestone.

Granite Mountain Batholith

The GMB is divided into four phases based on mineralogy and texture (Drummond et al., 1976; Ash et al., 1999b; van Straaten et al., 2013; Schiarizza, 2014, 2015). They are the Burgess Creek Stock, Granite Mountain Phase, Mine Phase, and the Border Phase (Fig. 1). Propylitic alteration, characterised by epidote and chlorite, is common in all four phases of the batholith with variable intensity. Phyllic alteration, identified by the occurrence of white mica and pyrite is limited to the Mine Phase, Border Phase and the south west section of the Granite Mountain Phase, proximal to mine pits. Quartz is abundant in rocks of the GMB as a primary mineral and a major component of various veins. The Granite Mountain Phase is the least altered and the Mine Phase and Border Phase are generally more altered based on abundances of pyrite, white mica, epidote and chlorite.

Burgess Creek Stock. The Burgess Creek Stock occurs at the northeast margin of the GMB (Fig. 1). It consists of tonalites, quartz diorites, and diorites that intrude the Nicola Group (Schiarizza, 2014). The tonalitic rocks of this phase are leucocratic with less than 10 vol.% mafic minerals. The dioritic rocks contain plagioclase (60-70 vol.%) and up to 30 vol.% mafic minerals. The Burgess Creek Stock was previously interpreted to be younger than the GMB (Panteleyev, 1978; Bysouth et al., 1995). This interpretation may be in part due to its intrusive contact with the Nicola volcanic rocks, which were previously considered younger than the GMB (Ash et al., 1999a, b). The stock yielded U-Pb zircon ages of 222.7 ± 0.3 Ma and 221.25 ± 0.2 Ma (Schiarizza 2015), which are older than the ages of the GMB. Ash et al (2001) reported 215 ± 0.8 Ma and Schiarizza (2015) obtained 217.15 ± 0.2 Ma from the adjacent Granite Mountain Phase of the batholith. These data suggest that the stock is an old unit of the GMB.

Granite Mountain Phase of the GMB. The Granite Mountain Phase is the most voluminous and most leucocratic phase of the GMB. This phase is equigranular and isotropic. It comprises tonalitic rocks with various modalities of quartz, plagioclase and minor chloritized mafic minerals (5-10 vol.%). The epidote content is low (<15 vol.%) and it replaces

plagioclase. U-Pb zircon ages date the Granite Mountain Phase of the GMB at 217 ± 0.2 Ma (Schiarizza, 2015).

Mine Phase of the GMB. The Mine Phase hosts the Cu-Mo mineralization at Gibraltar. It consists of tonalitic rocks with variable modalities of quartz, plagioclase and completely chloritized mafic minerals (15-25 vol.%). It is more leucocratic than the Border Phase. Rocks in this phase are highly foliated and equigranular. The epidote content ranges from 10-30 vol.%.

Border Phase of the GMB. The Border Phase comprises various modalities of quartz (up to 30 vol.%), plagioclase (up to 40 vol.%) and mafic minerals (up to 40 vol.%). Mafic minerals are hornblende \pm biotite and are partially to completely chloritized. It is equigranular and isotropic to slightly foliated. The epidote content is moderate (10-20 vol.%).

Sheridan Stock

The Sheridan Stock is composed of equigranular isotropic quartz diorite and tonalite (15-25 vol.% quartz, < 70 vol.% plagioclase, 10-20 vol.% mafic minerals). Pristine unaltered plagioclase, biotite and dark brown hornblende are common minerals of the stock. U-Pb zircon date, 108.1 ± 0.6 Ma (Ash et al., 2001), confirms the late Cretaceous age of the intrusion. Mafic minerals are dark brown hornblende and biotite with low (<10 vol.%) epidote content. Epidote-quartz veins generally strike east-west (Fig. 3A).

Analytical methods

SEM-EDS

Chemical compositions of epidote group minerals were determined from 12 carbon-coated polished thin sections using a JEOL 6610LV scanning electron microscope equipped with energy dispersive detector (SEM-EDS) at the University of Ottawa. The compositions were determined using energy-dispersive spectroscopy with the acquisition time of 40 s and an accelerating voltage of 20 kV. Analyses were conducted without references for individual elements. All detected element oxide values are

normalized to 100%. Detection limits are 0.1-0.5 wt% for all elements.

SEM back scattered electron (BSE) images were acquired as 16 bit greyscale. Up to 256 shades of grey were used to represent different mean atomic masses of different minerals and mineral compositions. These shades were converted to up to 30 colors using imageJ photo software by assigning each shade(s) of gray to a color. Brighter areas in gray scale BSE image within epidote grain represent higher Fe content. Blue, green and magenta were used to identify titanite, chlorite and chalcopyrite respectively, and separate these minerals from similar shades of grey in epidote. The gray color of apatite was left as the original color.

EPMA

Quantitative analysis for the major and minor elemental compositions of the epidote group minerals was carried out using a JEOL 8230 electron probe micro-analyzer (EPMA) at the University of Ottawa. Epidote minerals were analyzed at an accelerating voltage of 15 kV, a beam current of 20 nA using a focused beam of 1 μm . Counting times were 20 s on-peak and 10 s off-peak for all elements except for F (150 s on and 75 s off), Cl (50 s on and 25 s off), Y (40 s on and 20 s off) Sc (40 s on 20 s off), Si (10 s on and 5 s off). F, Cl Y, Sc, Th, Pb, Cr, Nb and K were all below detection levels for epidote analysis by EPMA and are not reported. References and limit of detections are indicated in Table 1.

Field observations

The orientation of 1 to 10 epidote-bearing veins were measured at 10 outcrops for a total of 50 measurements. Six out of 10 outcrops and 36 out of 50 measurements of epidote-bearing veins were in the GMB (Fig. 3A). The rest of the orientation measurements were taken on epidote-bearing veins in the Nicola volcanic rocks, the Sheridan Creek Stock or the Cuisson Lake Unit. The dominant orientation was determined after compiling all measurements from one outcrop. Typically, 80% of the veins at a site have a similar orientation with $\pm 5^\circ$ of variability which we consider the dominant orientation at the outcrop. The rest of the veins (about 20%) showed

variable strikes with more than 50° difference from the dominant vein orientation.

Epidote occurrences and composition

Nomenclature

Epidote group minerals with the general formula $A_2M_3(T_2O_7)(TO_4)(O,F)(OH,O)$ are divided into 3 subgroups: clinozoisite, allanite and dollaseite subgroups. The clinozoisite subgroup is defined by homovalent substitution of Al by Fe^{3+} in M sites. The allanite subgroup is defined by REE rich phases where trivalent REEs reside in the A site. The third subgroup is the dollaseite subgroup with high Mg and is not found in our study area. Ferriepidote, epidote and clinozoisite form a continuous solid solution in the clinozoisite subgroup with varying Fe^{3+} and Al in the M sites (Fig. 4). The endmember of clinozoisite has Al in three M sites. The endmember of epidote (*sensu stricto*) has Al in two M sites (M_1 and M_2) and Fe^{3+} in the M_3 site. The end-member ferriepidote has Fe^{3+} in two M sites (M_1 and M_3) and Al in the M_2 site (Armbruster et al., 2006) (Fig. 4). Epidote (*sensu stricto*) is defined to contain greater than 0.5 Fe^{3+} in the M_3 site, whereas clinozoisite contains greater than 0.5 Al in the M_3 site (Armbruster et al., 2006) (Fig. 4). Ferriepidote has a greater than 0.5 Fe^{3+} in the M_1 and the M_3 site is filled with Fe^{3+} (Armbruster et al., 2006). The $\text{Fe(t)}/[\text{Fe(t)} + \text{Al}]$ apfu ratios in the clinozoisite subgroup are > 0.5 for ferriepidote, 0.165-0.5 for epidote and < 0.165 for clinozoisite (Armbruster et al., 2006).

Allanite subgroup is defined to contain $[\text{M}^{3+} + \text{M}^{4+}]_{A2} > 0.5$ and $[\text{M}^{2+}]_{M3} > 0.5$, where M^{3+} and M^{4+} are REE, Y, U and Th substituting Ca^{2+} in the A_2 site and M^{2+} a divalent cation in the M_3 site to retain charge balance (Armbruster et al., 2006) (Fig. 4).

Epidote in the study area shows a large compositional variation mostly due to varying Fe, Al and REE contents. The atomic ratios of $\text{Fe(t)}/[\text{Fe(t)} + \text{Al}]$ are between 0.05 and 0.5 in studied samples and some grains also contain up to 21 wt.% $\text{La}_2\text{O}_3 + \text{Ce}_2\text{O}_3 + \text{Pr}_2\text{O}_3 + \text{Nd}_2\text{O}_3$.

Epidote in the GMB shows compositional zoning with Fe-poor cores and Fe-rich rims. The boundaries

Table 1. List of elements and references used for electron probe micro-analyzer.

Elements	References	Detection limits
Si, Al, K	Sanidine	Si (180 ppm), Al (100 ppm), K (130 ppm)
Fe	Hematite	Fe (150 ppm)
F	Mg-mica	F (390 ppm)
Na	Albite	Na (110 ppm)
Cl	Tugtupite	Cl (60 ppm)
Sr	Celestine	Sr (490 ppm)
Nd	Synthetic NdPO ₄	Nd (330 ppm)
Pr	PrPO ₄	Pr (640 ppm)
Ce	CePO ₄	Ce (380 ppm)
La	LaPO ₄	La (470 ppm)
Th	ThO ₂	Th (360 ppm)
Ca, Mg	Diopside	Ca (160 ppm), Mg (110 ppm)
Pb, V	Vanadinite	Pb (310 ppm), V (180 ppm)
Mn	Tephroite	Mn (440 ppm)
Y	Yttrium aluminium garnet	Y (2100 ppm)
Ti	Rutile	Ti (180 ppm)
Cr	Chromite	Cr (150 ppm)
Sc	REE-glass (synthetic glass with 1 wt.% of Sc)	Sc (200 ppm)
Nb	Synthetic manganocolumbite	Nb (540 ppm)

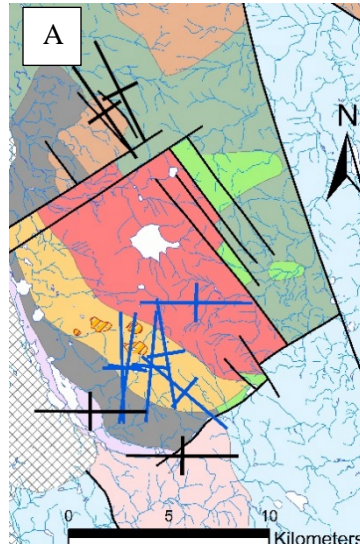


Figure 3 (A) Dominant orientations of epidote-bearing veins (greater than 2 cm in width) in the study area. Note dominant vein orientations in blue are in the GMB and veins strike east-west in the Granite Mountain Phase. Dominant vein orientations in black are not in the GMB. Colorized SEM-BSE

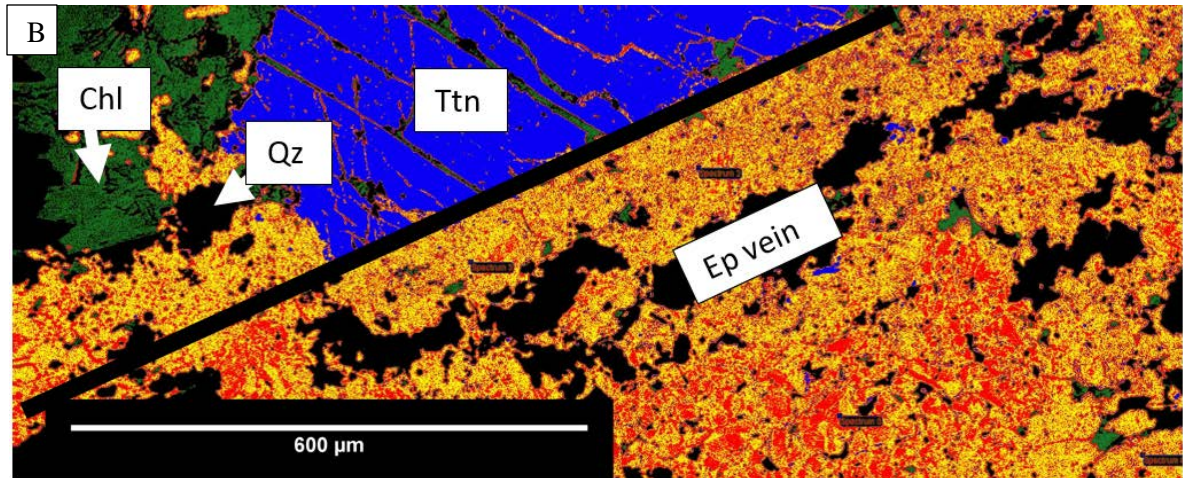


Figure 3. (B) Perpendicular to strike section of an Ep-Qz vein (1 cm in width) the Mine Phase of the batholith (sample GBR-2-7) comprising zoned epidote grains with Fe-poor centres (10.57 wt.% $\text{Fe}_2\text{O}_3(\text{t})$, $\text{Fe}(\text{t})/[\text{Fe}(\text{t}) + \text{Al}] = 0.21$) rimmed by Fe-rich borders (16.52 wt.% $\text{Fe}_2\text{O}_3(\text{t})$, $\text{Fe}(\text{t})/[\text{Fe}(\text{t}) + \text{Al}] = 0.33$). Epidote grains in the centre of the veins have large Fe-poor cores. Epidote grains on the border of veins have less prominent Fe-poor cores. Abbreviations: Chl – chlorite; Ep – epidote; Qz – quartz; Ttn – titanite. Sample locations and SEM data are found in Appendix Tables 1, 2 and 3

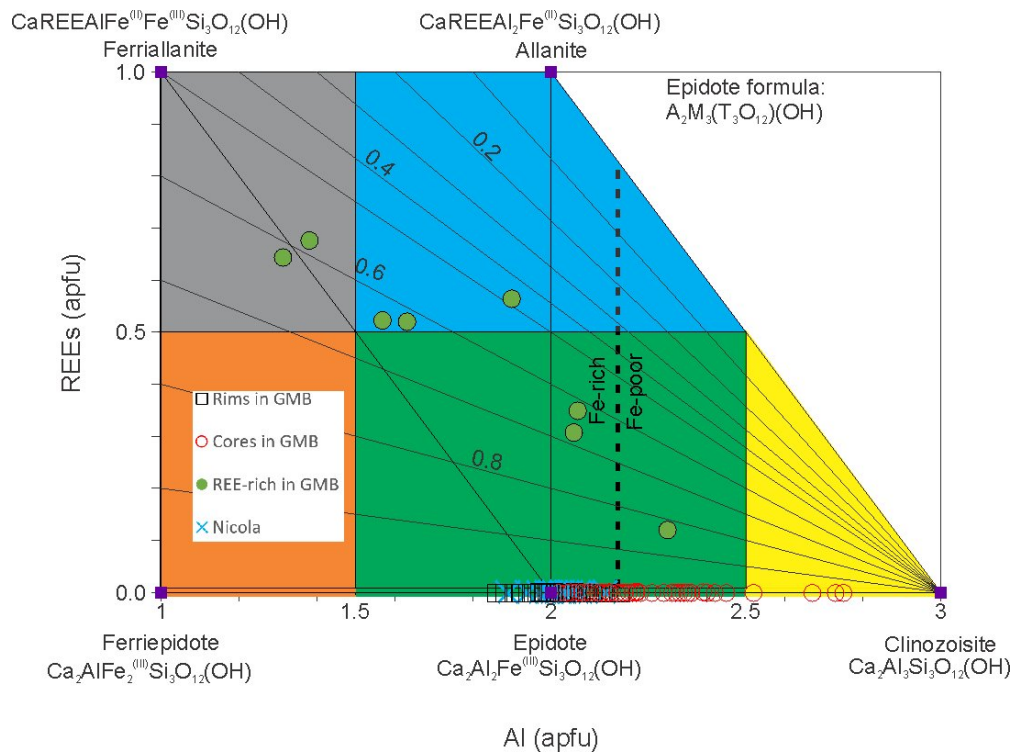


Figure 4: Total Al atoms per formula unit (apfu) vs. REEs (apfu) diagram showing solid solutions in the clinozoisite subgroup and the allanite subgroup after Petrik et al. (1995). Lines radiating from the clinozoisite end-member are $\text{Fe}^{3+}/(\text{Fe}^{3+} + \text{Fe}^{2+})$. End member compositions are shown as purple squares. Division of Fe-poor and Fe-rich epidotes in this study is shown with a dashed black line. The compositional ranges for epidote sensu stricto clinozoisite ferriepidote, allanite, and ferriallanite are shown as green, yellow, orange, blue and grey fields, respectively, following the classification of Armbruster et al. (2006).

between cores and rims are sharp in individual grains and there is no epidote with intermediate compositions. Based on our observation of Fe-Al zoning in epidote and clinozoisite of the GMB, we define “Fe-poor epidote” as having $\text{Fe(t)}/[\text{Fe(t)} + \text{Al}]$ ratios <0.29 and “Fe-rich epidote” with ratios >0.29 . In this study, REE+Y vary from 0.01 wt.% oxides to 21.7 wt.% oxides. We classify epidote as allanite (>15 wt.% REE oxides), REE-rich (1 to 15 wt.% REE oxides) and REE-bearing (0.01-1 wt.% REE oxides).

Epidote occurrences in the GMB

Disseminated epidote. Disseminated epidote in the GMB replaces 5 to 100 vol.% of plagioclase grains (Fig. 5). Individual grains of epidote in plagioclase have a tabular shape (Fig. 5) with up to 30 μm in length and show zoning with Fe-rich rims and Al-rich cores. Replacement of plagioclase by epidote occurs in all phases of the GMB. Total pseudomorphic replacement of plagioclase by aggregates of epidote grains (Fig. 6) is common only in the Mine Phase of the GMB.

Aggregates. Epidote forms aggregates (0.5 – 1 mm) consisting of small anhedral epidote grains (50-100 μm). Grains do not contain inclusions. The individual grains within the aggregates are zoned with Fe-rich rims and Al-rich cores. Aggregates are commonly surrounded by chlorite. Epidote aggregates occur in all phases of the GMB. Grains in some aggregates are REE-bearing.

Isolated grains. Epidote forms large (up to 400 μm) isolated grains associated with quartz phenocrysts. These grains are not associated with plagioclase or chlorite. The grains are euhedral to subhedral. Their composition ranges from Fe-poor epidote in the cores to Fe-rich epidote in the rims (Fig. 6). Some contain significant concentrations (>5 wt.%) of REE oxides (Fig. 7) and these REE-rich grains are not compositionally zoned. Isolated grains of epidote occur in all phases of the GMB.

Veins and veinlets. Epidote-bearing veins and veinlets occur in all phases of the GMB. Three types of veins (1-15 cm wide) and veinlets (0.1-3 mm wide) are observed: mono-mineralic epidote, epidote-quartz and epidote-quartz-chlorite. They contain

minor hydrothermal magnetite. Individual grains of epidote show compositional zoning with Fe-poor cores (Fig. 3). Thirty six measurements of vein orientation within the GMB show that they generally strike towards the mineralized areas (Fig. 3). Epidote-bearing veins are found up to 10 km from mineralization. This is farther than the disseminated epidote which extends < 5 km.

Epidote in ore zone in the Mine Phase of the GMB. Epidote grains in contact with, or in the proximity of pyrite or chalcopyrite (Figs. 8 and 9) are mostly subhedral and occur as aggregates (up to 600 μm) or isolated grains ranging from 50 to 400 μm . Grains enclosed by sulphides are unzoned, with low Fe ($\text{Fe(t)}/[\text{Fe(t)} + \text{Al}] < 0.22$) whereas those in contact, but not totally enclosed by sulphide minerals are partially zoned (Fig. 8).

REE-bearing epidote. REE-bearing (up to 0.2 wt% REE oxides) epidote occurs in all phases of GMB as aggregates and shows zoning with Fe-rich rims and Fe-poor cores in individual grains. Due to high detection limits of REEs, REE-bearing epidote was not detected with SEM-EDS. There is a higher proportion (54 %) of epidote that is REE-bearing in samples collected proximal to mine pits (<2 km). In contrast, samples collected far (>2 km) from mine pits have a lower proportion (25 %) of REE-bearing epidote grains.

Allanite and REE-rich epidote. Allanite and REE-rich epidote are only found in REE-rich (>70 ppm) rocks of the Mine Phase, Border Phase, and the Burgess Creek Stock of the GMB (Fig. 10). Grains of REE-rich epidote and allanite show patchy compositional variations with Ce_2O_3 contents ranging from 5 to 15 wt.%, La_2O_3 from 6 to 10 wt.%, Pr_2O_3 from 0.3 to 1 wt.% and Nd_2O_3 from 0.4 to 1.3 wt.%. No Fe-Al zoning is observed in REE-rich epidote or allanite (Fig. 7).

Epidote in the Nicola volcanic rocks

Epidote occurs as large isolated subhedral grains (up to 400 μm , Fig. 5), and as aggregates (up to 500 μm) of small (<50 μm) grains. Epidote grains and aggregates are commonly associated with chlorite. Grains are homogeneous in composition and classify

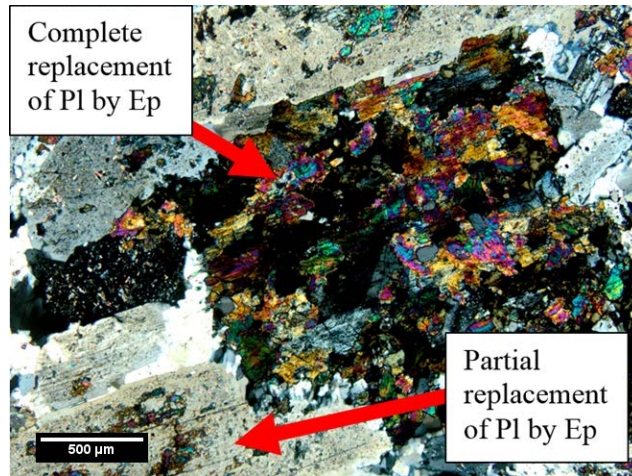


Figure 5. Photomicrograph showing variable degrees of replacement of plagioclase (Pl) by epidote (Ep) in the GMB. Sample number GBR-16 from the Mine Phase of the GMB, sample locations are listed in Appendix Table 1.

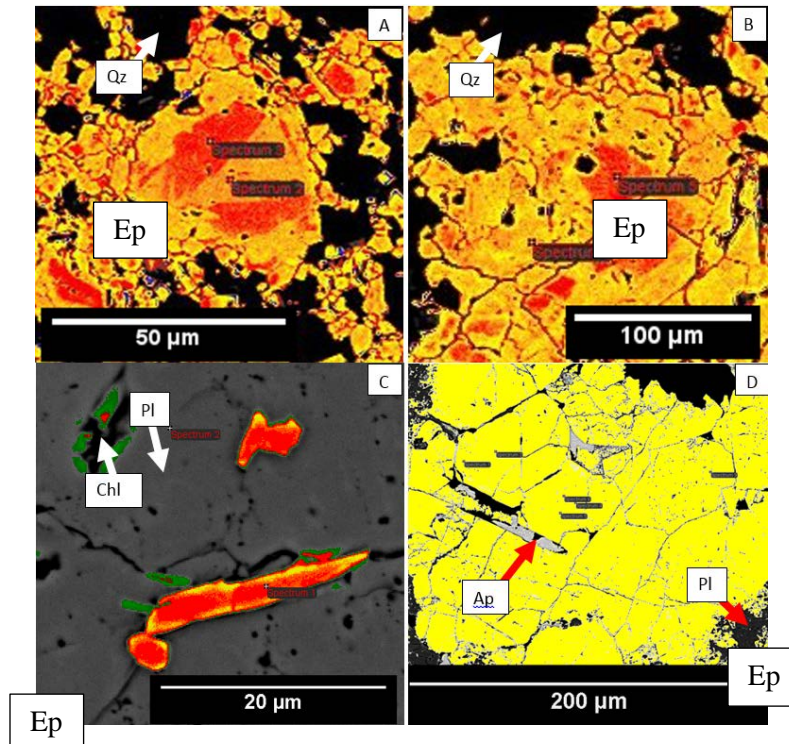


Figure 6. Colorized scanning electron microscopy-back scattered electron image (BSE) of epidote (Ep) surrounded by quartz (Qz) and plagioclase (Pl) in tonalitic rocks of the batholith (A, B, C) and epidote in Nicola volcanic rocks surrounded by plagioclase (D). (A) Ep aggregate in Mine Phase of the batholith showing Fe-poor cores (red, 10.07 wt.% $\text{Fe}_2\text{O}_3(\text{t})$, $\text{Fe}(\text{t})/[\text{Fe}(\text{t}) + \text{Al}] = 0.2$) and Fe-rich rims (yellow, 16.03 $\text{Fe}_2\text{O}_3(\text{t})$ wt.%, $\text{Fe}(\text{t})/[\text{Fe}(\text{t}) + \text{Al}] = 0.31$); sample GBR2-10; (B) Isolated Ep grain in the Border Phase of the batholith showing Fe-poor cores (red, 11.97 $\text{Fe}_2\text{O}_3(\text{t})$ wt.%, $\text{Fe}(\text{t})/[\text{Fe}(\text{t}) + \text{Al}] = 0.24$) and Fe-rich rims (yellow, 18.72 $\text{Fe}_2\text{O}_3(\text{t})$ wt.%, $\text{Fe}(\text{t})/[\text{Fe}(\text{t}) + \text{Al}] = 0.36$); sample GBR2-8; (C) Disseminated Ep in Granite Mountain Phase of the batholith showing Fe-poor cores (red, 8.74 $\text{Fe}_2\text{O}_3(\text{t})$ wt.%, $\text{Fe}(\text{t})/[\text{Fe}(\text{t}) + \text{Al}] = 0.17$) and Fe-rich rims

Figure 6. Continued. (yellow, 18.53 Fe₂O₃(t) wt.%, Fe(t)/[Fe(t) + Al] = 0.36); sample GBR2-34; (D) Isolated Fe-rich (17.56 Fe₂O₃(t) wt.%, Fe(t)/[Fe(t) + Al] = 0.34) epidote grain in the Nicola volcanics showing no zoning and inclusions of apatite (Ap). Sample GBR2-4. Abbreviations; Chl – chlorite, sample locations and SEM data are found in Appendix Tables 1, 2, 3, and 4.

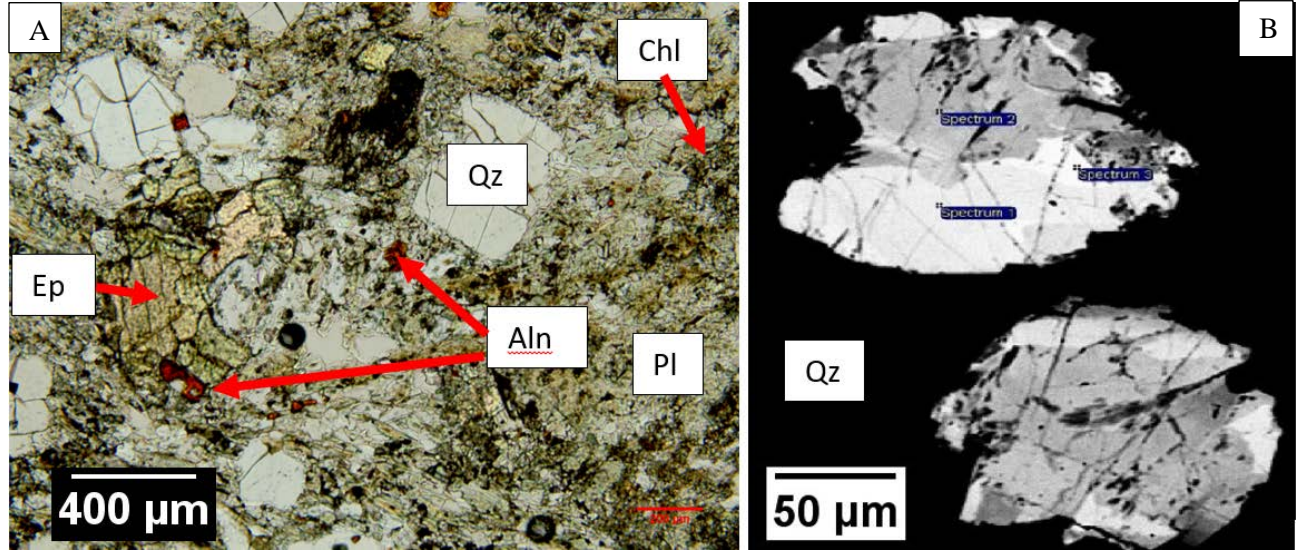


Figure 7. (A) Photomicrograph under open polarizers and (B) SEM –BSE image of allanite in the Mine Phase of the GMB; sample GBR-11. (A) Allanite (Aln, red-orange grains) surrounded by Ep, Qz and Chl. (B) Patchy zoning in allanite with brighter areas with Ce₂O₃ > 10 wt.% and darker areas with Ce₂O₃ < 5 wt.%. Sample location and SEM data found in Appendix Tables 1 and 5.

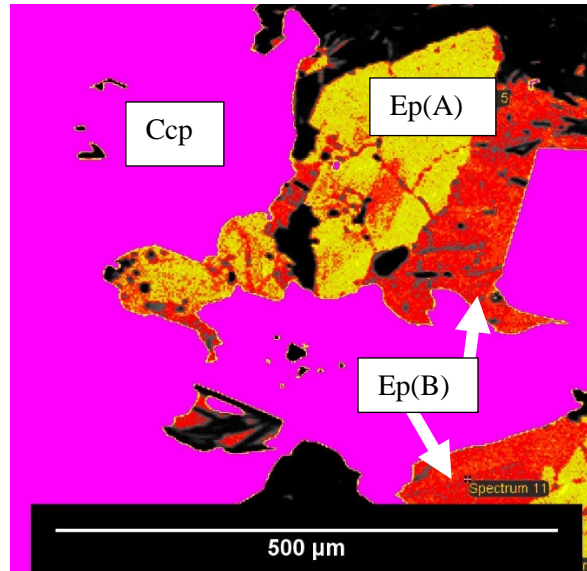


Figure 8. Colorized SEM-BSE of epidote (Ep) in contact with chalcopryite (Ccp, pink) in sample SVA 7-14.13, collected in the Mine Phase of the GMB. Zoning with relatively Fe-rich rims (yellow, 13.15 wt.% FeO(t), Fe(t)/[Fe(t) + Al] = 0.25) and Fe-poor-cores (11.02 wt.% Fe₂O₃(t), Fe(t)/[Fe(t) + Al] = 0.21) in Ep(A) in contact but not surrounded by Ccp. Ep (B) enclosed by Ccp shows no zoning and is Fe-poor (11.53 wt.% Fe₂O₃(t), Fe(t)/[Fe(t) + Al] = 0.23). Sample location and SEM data found in Appendix Tables 1 and 8.

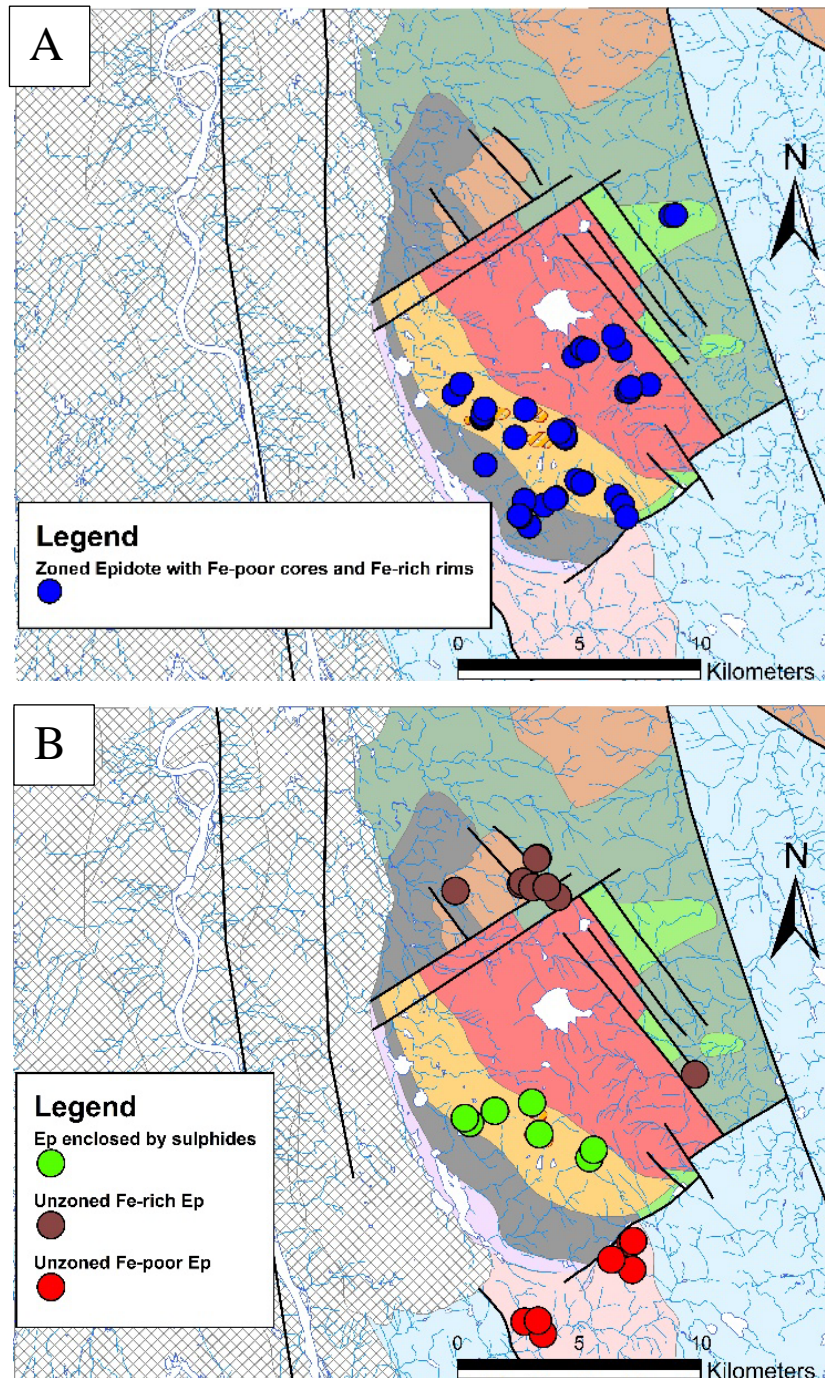


Figure 9. (A) Location of zoned epidote (Fe-poor cores and Fe-rich rims) in the Border Phase, Mine Phase, Granite Mountain Phase, and Burgess Creek Stock of the GMB. (B) Location of unzoned epidote in the study area. Fe-rich unzoned epidote is found in the Nicola volcanic rocks (brown), Fe-poor unzoned epidote is found in disseminated epidote replacing plagioclase in the Sheridan Creek Stock. Unzoned Fe-poor epidote is found in the Mine Phase where enclosed in sulphides.

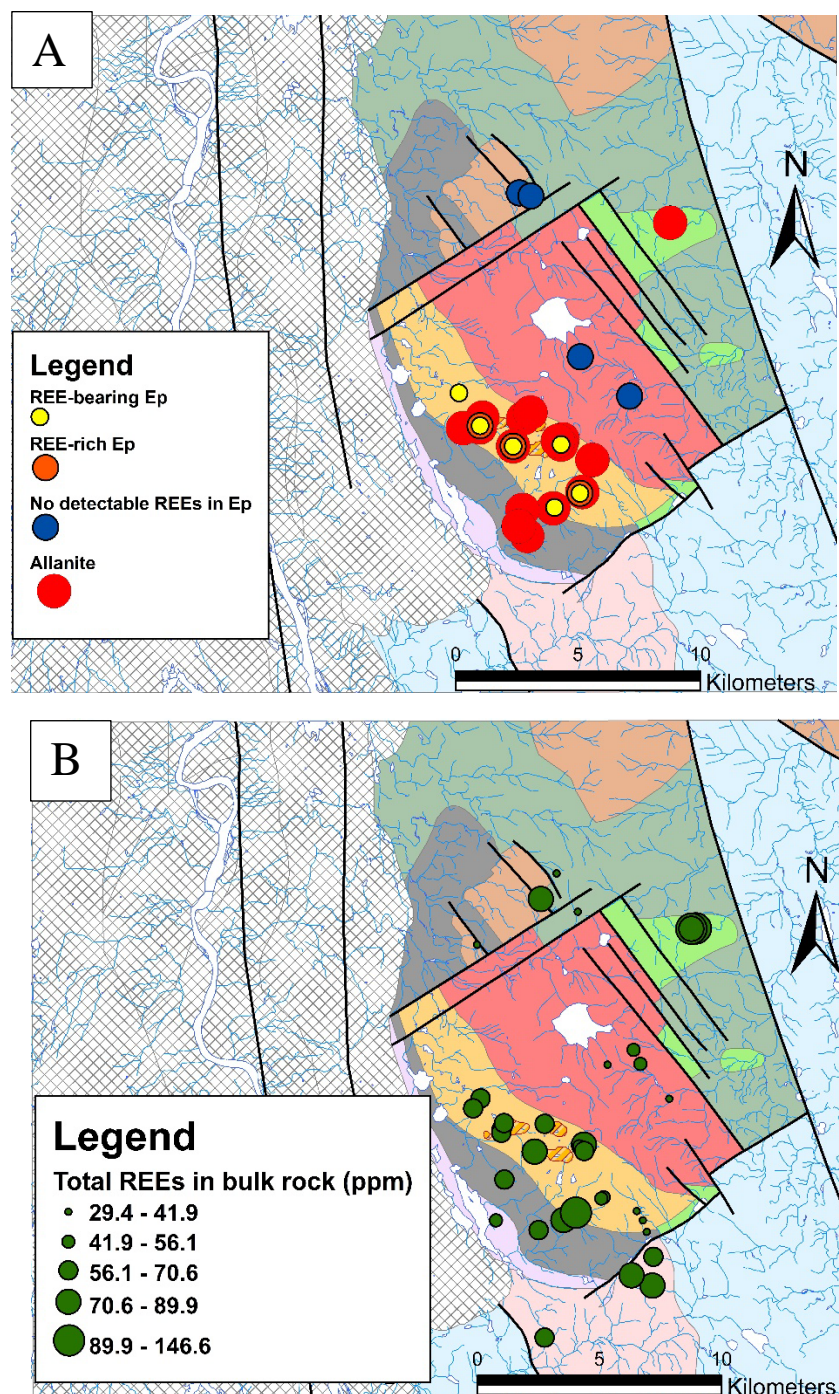


Figure 10. (A) Location of zoned epidote (Fe-poor cores and Fe-rich rims) in the Border Phase, Mine Phase, Granite Mountain Phase, and Burgess Creek Stock of the GMB. (B) Location of unzoned epidote in the study area. Fe-rich unzoned epidote is found in the Nicola volcanic rocks (brown), Fe-poor unzoned epidote is found in disseminated epidote replacing plagioclase in the Sheridan Creek Stock. Unzoned Fe-poor epidote is found in the Mine Phase where enclosed in sulphides.

as Fe-rich. The larger isolated grains commonly contain apatite and titanite inclusions (Fig. 5). Nicola volcanic rocks near (< 500 m) the contact with the GMB contain more epidote (>40 vol.%) than volcanic rocks far (>500 m) from the GMB, which contain less than 30 vol.% epidote. Epidote in Nicola volcanic rocks does not contain REEs above the detection limits of SEM and EPMA. Tables 2 and 3 present a summary of epidote composition in the GMB and the Nicola volcanic rocks.

Epidote in the Sheridan Creek Stock

Disseminated epidote replacing plagioclase is present in the Sheridan Creek Stock. Epidote modalities are lower in the Sheridan Creek Stock (~ 5-10 vol.%) compared to that in the GMB (>10 vol.%).

Epidote in the Cuisson Lake Unit

In the Cuisson Lake Unit, epidote occurs in wide (>5 cm) deformed veins of epidote, epidote-quartz and epidote-calcite. Coarse grained epidote also occurs in lenses along with calcite (Fig. 2). Epidote and chlorite are major components of the fine grained matrix of the Cuisson Lake unit. In total, epidote constitutes up to 40 vol.% of this unit.

Discussion

Epidote in the batholith

Epidote occur in all phases of the GMB (Fig. 10). A $\text{Fe(t)}/[\text{Fe(t)} + \text{Al}]$ value of 0.29 separates compositions of cores from rims for individual epidote grains (Fig. 11). Epidote enclosed by chalcopyrite and pyrite is homogeneous and Fe-poor suggesting the preferential incorporation of Fe in sulfides. All other epidote in the GMB shows compositional zoning; Fe-poor, Al-rich cores and Fe-rich, Al- poor rims (Fig. 9). We interpret this zoning as reflecting early S-rich hydrothermal activity that produced pyrite and chalcopyrite, leaving the associated epidote relatively low in Fe. Later hydrothermal activity with relatively less S did not form sulphides leaving Fe enriched fluids for the formation of Fe-rich rims in epidote.

REE-bearing epidote, REE-rich epidote and allanite in the batholith

REE-bearing epidote occurs in all phases of the GMB, except in the Granite Mountain Phase (Fig. 9A). Minute grains forming epidote aggregates commonly contain REEs, but the contents are lower than 1 wt.% REE oxides. On the other hand, all grains of REE-rich epidote and allanite form isolated grains. REE-rich epidote and allanite are restricted within the GMB (Fig. 9). They are a hydrothermal product. The presence of allanite and REE-rich epidote only in rocks that contain >70 ppm REEs suggest that the rocks and epidote were enriched in light REE during hydrothermal activity or that the original rocks contain high REEs. The allanite subgroup has the potential to substitute Y, U and Th. Allanite and REE-rich epidote in this study do not have detectable Y, U or Th.

Epidote veins in the batholith

Veins of epidote are common throughout the batholith and extend up to 10 km from mineralization. Some are monomineralic, some are epidote-quartz or epidote-quartz-chlorite. Epidote grains in veins carry the same zoning pattern as observed in hydrothermal epidote of the GMB indicating that the veins were produced by the hydrothermal activity for crystallization of disseminated epidote. Although the number of measurements on vein orientations is limited (N=36), the dominant orientation at each site generally strike towards the centre of the mineralization (Fig. 3A). If this is proven to be the case, epidote vein orientation in an intrusion could serve to vector towards mineralization.

Epidote in Nicola volcanics

We suggest that epidote in the Nicola volcanic rocks near the GMB is a contact metamorphic product related to the intrusion of GMB, based on high abundance of epidote close to the contact with the GMB and that epidote in the Nicola volcanic rocks does not share the zoning pattern or composition of epidote in the GMB. Alternatively, increase in epidote modality near the contact may be due to enhanced fluid flow along the contact between the Nicola volcanic rocks and the GMB. Nicola epidote plots as

Table 2. Summary, compositional zoning of epidote grains in the GMB based on SEM-EDS and EPMA determinations.

Occurrence	Zoning in individual grains	Fe₂O₃ (t) (wt.%) rims [number of grains analyzed]	Fe₂O₃(t) (wt.%) cores [number of grains analyzed]
Enclosed by Ccp or Py	No zoning Al-rich	13.9 - 9.96 [3]	
In contact with Ccp or Py	Fe-rich rims, Al- rich cores	15.5 – 13.8 [5]**	9.8 – 12.3 [6]**
In veins*	Fe-rich rims, Al-rich cores	16.6 - 14.6 [13]**	12.5 -10.7[17]**
Isolated grains/ Grains within aggregates	Fe-rich rims, Al- rich cores	15.3 -13.8[24]**	8.4 - 10.9[27]**
Disseminated	Fe-rich rims, Al- rich cores	14.3 – 12.8 [7] **	2.1 – 9.4 [12] **

**Epidote grains in veins are zoned

**Presence of compositional zoning was apparent in all grains of epidotes in thin section under crossed polarizing light and also in SEM-BSE images. Only a small number of representative grains were selected for the composition analysis.

Table 3. Summary, epidote composition in Nicola volcanics based on SEM-EDS and EPMA determinations.

Occurrence	Zoning of grains	Fe₂O₃ (t) (wt.%) average [number of grains analyzed]	Inclusions
Isolated grains	None	15.3[10]**	Apatite and titanite
Aggregates	None	15.5[7]**	Not present

**Presence of compositional zoning was absent in all grains of epidotes in thin section under crossed polarizing light and also in SEM-BSE images. Only a small number of representative grains were selected for the composition analysis.

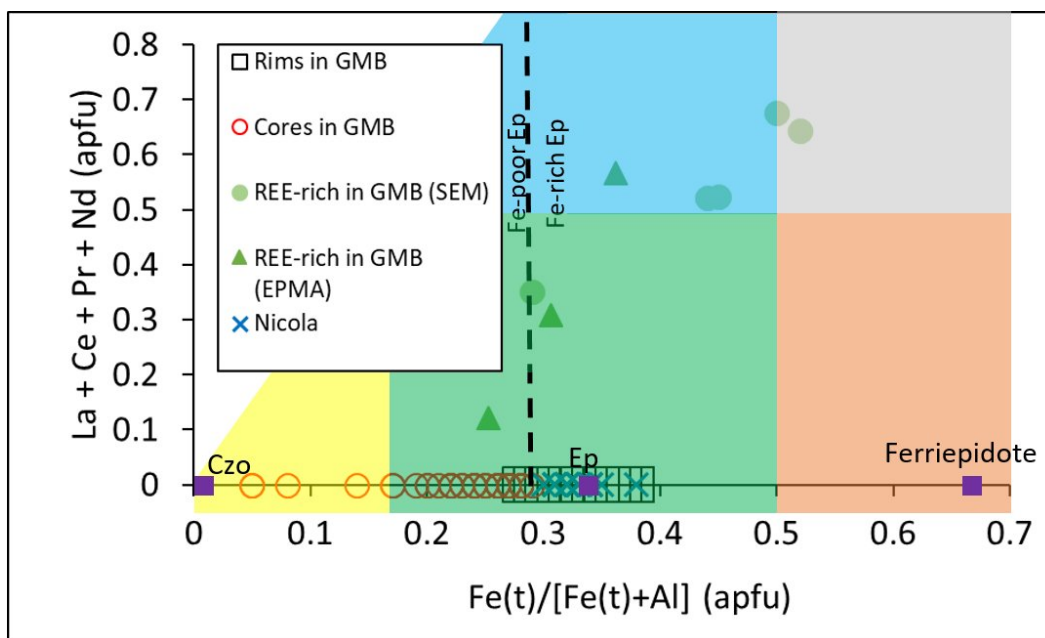


Figure 11. Composition of epidote in the GMB and the Nicola volcanic rocks based on SEM and EPMA data. Atom per formula unit calculated based on 12.5 O. End member compositions of clinozoisite (Czo, $\text{Ca}_2\text{Al}_3\text{Si}_3\text{O}_{12}(\text{OH})$), epidote (Ep, $\text{Ca}_2\text{Al}_2\text{Fe}^{(\text{III})}\text{Si}_3\text{O}_{12}(\text{OH})$) and ferriepidote ($\text{Ca}_2\text{AlFe}_2^{(\text{III})}\text{Si}_3\text{O}_{12}(\text{OH})$) are shown as purple squares. Ranges for clinozoisite (yellow field), epidote (green field), ferriepidote (orange field), allanite (blue field) and ferriallanite (grey field) following the nomenclature and classification of Armbruster et al. (2006). This paper classifies epidote as Fe-rich or Fe-poor with a boundary at 0.29 $\text{Fe}(\text{t})/[\text{Fe}(\text{t}) + \text{Al}]$ shown by the dashed black line. Fe-poor epidote includes clinozoisite. Epidote in Nicola volcanic rocks are all Fe-rich, $>0.29 \text{ Fe}(\text{t})/[\text{Fe}(\text{t}) + \text{Al}]$ ratios. REE-rich epidote and allanite contain Fe^{2+} and have ratios of $\text{Fe}(\text{t})/[\text{Fe}(\text{t}) + \text{Al}] > 0.24$.

Fe-rich (Fig. 11). Fe-rich composition of epidote may be explained by fluids interacting with mafic volcanic rocks because Fe/Al ratios are higher in mafic volcanic rocks compared to tonalitic rocks of the GMB.

Summary

Epidote in the GMB shows a variety of textures, occurrences, compositions and forms: pseudomorphic replacement of plagioclase, dissemination in plagioclase, aggregates, isolated grains, veins and veinlets. Epidote grains in the GMB contain no mineral inclusions. Almost all grains show a zoning pattern with Fe-rich rims and Al-rich cores except for grains enclosed by sulphides, REE-rich epidote and allanite. Grains enclosed by sulphides are all Fe-poor and REE-rich epidote and allanite are mostly Fe-rich.

REE-bearing epidote (0.01-1 wt.% REE oxides) occur as pseudomorphic replacement of plagioclase, dissemination replacing plagioclase, aggregates, isolated grains, veins and veinlets and is found in all phases of the batholith. It shows the same compositional zoning as epidote in the GMB and contains no mineral inclusions.

REE-rich epidote (1-15 wt.% REE oxides) and allanite are found in REE-rich (>70 ppm) rocks in the GMB, dominantly at less than 2 km from the mineralization and in the Burgess Creek Stock at >10 km from mineralization. REE-rich epidote also occurs in the Burgess Creek Stock, the oldest phase of the batholith. REE-rich epidote occurs only in REE-rich rocks suggesting that host rocks were originally rich in REE or hydrothermal enrichment in REEs contributed to the formation of REE-rich epidote and allanite.

Strike and dip measurements on a limited number of epidote veins in the GMB (N=36) indicate a general pattern of veins striking towards mineralization (Fig. 3A). If proven right, epidote vein orientation could be a vectoring tool in mineral exploration.

The Al-Fe zoning found in most epidote grains from the GMB is not observed in epidote from the unmineralized Nicola volcanic rocks. Epidote grains in the Nicola volcanic rocks are Fe-rich and have similar compositions independent of the locations. They commonly contain inclusions of apatite and titanite. Their REE content is below detection limits of 470 ppm for La, 380 ppm for Ce, 640 ppm for Pr and 330 ppm for Nd.

Epidote could be a useful indicator mineral for porphyry Cu mineralization if epidote found in nearby sediments has the signature of the mineralization and if it can be traced to mineralization. Another use of epidote in exploration is mapping of vein orientations and frequency in outcrops. If epidote veins show similar signatures (consisting of zoned grains as described above), they could be used to vector towards mineralization if the strike and dip pattern discussed in this report is proven to be correct.

Acknowledgements

This project was funded by Natural Resources of Canada through the Targeted Geoscience Initiative 5 program including a Research Affiliate Program Bursary to C.K. We also thank Glenn Poirier of the University of Ottawa for his help with SEM and EMPA analyses. The manuscript was improved following the internal GSC review completed by S.E. Jackson.

Appendix

Table 1. GPS locations for all samples in this study using NAD 83

Table 2. Composition of epidote rims in the GMB based on SEM-EDS analyses.

Table 3. Composition of epidote cores in the GMB based on SEM-EDS analyses.

Table 4. Composition of epidote in Nicola volcanics based on SEM-EDS analyses.

Table 5. Composition of REE-rich epidote and allanite in the GMB based on SEM-EDS analyses.

Table 6. Composition of epidote rims in the GMB based on EPMA analyses.

Table 7. Composition of epidote cores in the GMB based on EPMA analyses.

Table 8. Composition of REE-rich epidote in the GMB based on EPMA analyses.

Table 9. Compositions of epidote in contact with pyrite or chalcopyrite in the GMG based on SEM-EDS analyses.

References

- Armbruster, T. et al., 2006. Recommended nomenclature of epidote-group minerals; *European Journal of Mineralogy*, v. 18, p. 551-567.
- Ash, C.H., and Riveros, C.P., 2001. Geology of the Gibraltar copper molybdenite deposit, east-central British Columbia (93B/9); *in: Geological Fieldwork 2000*, British Columbia Ministry of Energy and Mines, British Columbia Geological Survey, Paper 2001-1, p. 119-133.
- Ash, C.H., Rydman, M.O., Payne, C.W., and Panteleyev, A., 1999a. Geological setting of the Gibraltar mine, south-central British Columbia (93B/8, 9); *in: Exploration and Mining in British Columbia 1998*, British Columbia Ministry of Energy and Mines, p. A1-A15.
- Ash, C.H., Panteleyev, A., MacLennan, K.L., Payne, C.W., and Rydman, M.O., 1999b. Geology of the Gibraltar mine area, NTS 93B/8, 9; British Columbia Ministry of Energy and Mines, British Columbia Geological Survey Open File 1999-7; scale 1:50 000.
- Ash, C.H. and Riveros, C.P., 2001. Geology of the Gibraltar copper-molybdenite deposit, east-central British Columbia (93B/9); *in: Geological Fieldwork 2000*, British Columbia Ministry of Energy and Mines, Paper 2001-1, p. 119-134.
- Bysouth, G.D., Campbell, K.V., Barker, G.E., and Gagnier, G.K., 1995. Tonalite-trondhjemite

- fractionation of peraluminous magma and the formation of syntectonic porphyry copper mineralization, Gibraltar mine, central British Columbia; *in*: Porphyry Deposits of the Northwestern Cordillera of North America, (ed.) T.G. Schroeter; Canadian Institute of Mining, Metallurgy and Petroleum, Special Volume 46, Montréal, p. 201-213.
- Colpron, M. and Nelson, J.L., 2011. A digital atlas of terranes for the Northern Cordillera; British Columbia Ministry of Energy and Mines, British Columbia Geological Survey, GeoFile 2011-11.
- Drummond, A.D., Sutherland Brown, A., Young, R.J., and Tennant, S.J., 1976. Gibraltar - Regional metamorphism, mineralization, hydrothermal alteration and structural development; *in*: Porphyry Deposits of the Canadian Cordillera, (ed.) A. Sutherland Brown; Canadian Institute of Mining and Metallurgy, Special Volume 15, p. 195-205.
- Panteleyev, A., 1978. Granite Mountain project (93B/8); *in*: Geological Fieldwork 1977, British Columbia Ministry of Energy and Mines, British Columbia Geological Survey, Paper 1978-1, p. 39-42.
- Petrík, I., Broska, I., Lipka, J., and Siman, P., 1995. Granitoid allanite-(Ce): substitution relations redox conditions and REE distributions (an example of I-type granitoids, Western Carpathians, Slovakia); *Geologica Carpathica*, v. 46, p. 79-94.
- Plouffe, A., and Ferbey, T., 2015. Till composition near Cu-porphyry deposits in British Columbia: Highlights for mineral exploration; *in*: TGI 4 - Intrusion Related Mineralisation Project: New Vectors to Buried Porphyry-Style Mineralisation, (ed.) N. Rogers; Geological Survey of Canada, Open File 7843, p. 15-37.
- Schiarizza, P., 2014. Geological setting of the Granite Mountain batholith, host to the Gibraltar porphyry Cu-Mo deposit, south-central British Columbia; *in*: Geological Fieldwork 2013, British Columbia Ministry of Energy and Mines, British Columbia Geological Survey, Paper 2014-1, p. 95-110.
- Schiarizza, P., 2015. Geological setting of the Granite Mountain batholith, south-central British Columbia; *in*: Geological Fieldwork 2014, British Columbia Ministry of Energy and Mines, British Columbia Geological Survey Paper 2015-1, p. 19-39.
- Sillitoe, R.H., 2010. Porphyry Copper Systems; *Economic Geology*, v. 105, p. 3-41.
- van Straaten, B.I., Oliver, J., Crozier, J., and Goodhue, L., 2013. A summary of the Gibraltar porphyry copper-molybdenum deposit, south-central British Columbia, Canada; *in*: Porphyry Systems of Central and Southern British Columbia: Tour of Central British Columbia Porphyry Deposits from Prince George to Princeton, (eds.) J.M. Logan and T.G. Schroeter; Society of Economic Geologists, Field Trip Guidebook, Series 43, p. 55-66.